Diffusion in a one-dimensional system with nearest and next-nearest neighbor interactions: Exact analysis based on the kinetic lattice gas model

S. H. Payne and H. J. Kreuzer

Department of Physics and Atmospheric Science, Dalhousie University, Halifax, NS B3H 3J5 Canada

From the master equation we derive the equation for the time evolution of the local density in terms of correlation functions. In the long-time and large-scale limit we use a gradient expansion together with the assumption of local equilibrium to derive an analytical expression for the density and temperature dependence of the diffusion coefficient. For various choices of the detailed kinetics and with the inclusion of first and second neighbor and trio interactions we show explicitly that the Reed-Ehrlich factorization holds exactly, we give explicit results and discuss their implications for the understanding of experimental results. We compare our method to existing analytic approaches and indicate its extensions.

PACS number(s): 68.43.De, 68.43.Jk

I. INTRODUCTION

Various theoretical approaches have been applied to the study of diffusion in low-dimensional systems, from analytic methods based on the master, Fokker-Planck, or Kramers equations, to numerical methods based on Monte Carlo and molecular dynamics simulations. The former provide physical insight, though usually at the cost of some simplifying assumptions, and closed form solutions in special cases. Simulation methods have the advantage of producing realistic, though numerical, results for particular physical systems. Several reviews exist, together covering all these approaches.[1–5] Required for all methods is a representation of the dynamics of the diffusing particle. For particles moving between well defined lattice sites the energy barrier can be calculated accurately by *ab initio* methods. However, this alone does not determine the dynamics[5] and approximations to the latter must be made, short of full-blown quantum-mechanical treatments.[6,7]

Diffusion, both tracer and collective, on the basis of the lattice gas model has been studied since the pioneering work of Elliott.[2,8] For this description the usual starting point is the master equation with the hopping between lattice sites treated as a Markovian process, i.e., the residence time at sites is long compared to the time of individual hops. This is also the easiest route to incorporate the effects of multiple binding sites within cells and particle interactions, both hardcore within cells and short range between them. In the case of surface diffusion such interactions lead to a strong dependence of the diffusivity on the coverage of the ad species. The "dynamics" in this kinetic lattice gas model are usually simplified to the specification of transition probabilities with a hopping rate, usually of an Arrhenius form, but modified by interactions with neighboring particles in the initial and final configurations, leading to vastly different diffusion behavior.[1]

Except in some special cases, e.g., hardcore exclusion alone, analytic solutions for the diffusivity do not exist and calculations are usually made using linear response theory or Monte Carlo simulations. A number of solutions for the coverage dependence of the collective diffusion coefficient in a one-dimensional (1D) system has been obtained, e.g., by Zwerger[9] using linear response theory, and by Gortel *et al.*[10] using a variational method for the diagonalization of the transition rate matrix. Another type of approach is based on gradient expansions of correlators as originally pioneered by Kawasaki[11] and Kikuchi[12,13] with some further developments, e.g., Chvoj.[14] Recently, an exact solution of the complete nonequilibrium time evolution of a finite 1D lattice gas with nearest neighbor interactions has been obtained by exact diagonalization in momentum space with the diffusivity emerging in the hydrodynamic limit.[15]

Although diffusion in a 1D lattice model has been addressed several times there does not exist a rigorous and transparent treatment in the sense that either approximate methods were used or unnecessary restrictions to hopping kinetics and static interaction scenarios were imposed. In this paper we will show that with a transparent method the coverage dependence of the collective (or chemical) diffusivity can be derived exactly for all choices of kinetics and lateral interactions of any desired range. The method used is a straightforward gradient expansion of all the correlators in the diffusion current. This method lends itself naturally to prove that the diffusivity follows the Reed-Ehrlich factorization[16] into a product of a thermodynamic factor (inverse susceptibility) and a kinetic factor (average hopping rate). This result clearly shows that the usual restrictions imposed on the kinetics for the use of linear response theory, namely that particle currents must vanish, is not needed and misleading. The methods developed here for a general 1D system lend themselves straightforwardly to an extension to 2D systems.

This paper is structured as follows. In the next section we present the elements of the kinetic lattice gas model which leads naturally to the equation of motion of the density and by a gradient expansion to Fick's law, done in Sec. III for nearest neighbor interactions only. The result is an explicit formula for the coverage dependence of the diffusivity in terms of local equilibrium correlation functions. The Reed-Ehrlich factorization is proven analytically. In Sec. IV we present a number of different diffusion scenarios, again restricted to nearest neighbor interactions. The generalization to second neighbor pair and trio interactions is then given in Sec. V. Although the number of plausible hopping scenarios

is an order of magnitude larger, everything can still be done analytically; in particular the Reed-Ehrlich factorization is still valid. The complexity of the diffusivity is demonstrated in a number of explicit examples in Sec. VI. We conclude with a discussion of our approach and its relation to previous work. Some details of our method are collected in two appendixes.

II. KINETIC LATTICE GAS MODEL

To set up the kinetic lattice gas model, one assumes that the surface of a solid can be divided into N_s cells labeled i, for which one introduces microscopic occupation numbers $n_i=1$ or 0, depending on whether cell i is occupied by an adsorbed particle or not. There are 2^{N_s} microstates $\mathbf{n} = (n_1, n_2, \ldots, n_{N_s})$ given by sequences of zeroes and ones. To introduce the dynamics of the system one writes down a model Hamiltonian, here in one dimension,

$$H(\mathbf{n}) = E_s \sum_i n_i + V_1 \sum_i n_i n_{i+1} + V_2 \sum_i n_i n_{i+2} + \cdots . \quad (1)$$

Arguing that the lattice gas Hamiltonian should give the same Helmholtz free energy as a microscopic Hamiltonian (for noninteracting particles) one can show that the proper identification of E_s is the free energy per particle[17]

$$E_s = -V_0 - k_B T \ln(q_3 q_{\text{int}}) \quad (2)$$

with V_0 the depth of the surface potential. The center-of-mass vibrations of the adsorbed molecule in this potential well are represented by the partition functions $q_3 = q_z q_{xy}$, with normal (z) and in-plane (x,y) components; $q_{\text{int}} = q_{\text{vib}} q_{\text{rot}}$ is the partition function for the internal degrees of freedom (vibrations, ν_v and hindered rotations, ν_r). These modes are usually described by 1D harmonic oscillators. V_1, V_2 are interactions between first and second nearest neighbor particles.

We introduce a function $P(\mathbf{n},t)$ which gives the probability that a given microstate $\mathbf{n}$ is realized at time t and define the transition probability $W(\mathbf{n},\mathbf{n}')$ per unit time as the probability to go from a state $\mathbf{n}'$ to $\mathbf{n}$. Treating diffusion as a Markov process $P(\mathbf{n},t)$ must satisfy a master equation

$$\frac{dP(\mathbf{n},t)}{dt} = \sum_{\mathbf{n}'} [W(\mathbf{n},\mathbf{n}')P(\mathbf{n}',t) - W(\mathbf{n}',\mathbf{n})P(\mathbf{n},t)]. \quad (3)$$

To ensure the approach to equilibrium in an isolated system each term in the sum must satisfy detailed balance

$$W(\mathbf{n},\mathbf{n}')P_{\text{eq}}(\mathbf{n}') = W(\mathbf{n}',\mathbf{n})P_{\text{eq}}(\mathbf{n}), \quad (4)$$

where

$$P_{\text{eq}}(\mathbf{n}) = \frac{e^{[-H(\mathbf{n})-\mu N(\mathbf{n})]/k_B T}}{\Xi}, \quad (5)$$

$$\Xi = \sum_{\mathbf{n}} e^{[-H(\mathbf{n})-\mu N(\mathbf{n})]/k_B T} \quad (6)$$

is the equilibrium probability and Ξ is the grand canonical partition function. In principle, $W(\mathbf{n}',\mathbf{n})$ must be calculated from a Hamiltonian that includes, in addition to Eq. (1), cou-
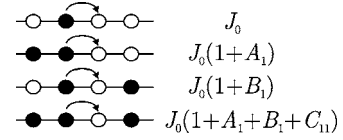

FIG. 1. The four relevant hopping processes and their rates for a one-dimensional lattice gas with nearest neighbor interactions.

pling terms to the gas phase and the solid phase that mediate mass and energy exchange. In this paper we will rather follow the procedure initiated by Glauber[18] in setting up the kinetic Ising model and guess the appropriate form of $W(\mathbf{n}',\mathbf{n})$.

If we treat the diffusion as the result of particles hopping from an occupied site to a neighboring unoccupied site we can write the transition probability as[19]

$$W_{\text{diff}}(\mathbf{n}',\mathbf{n}) = \sum_i [W_i^>(\mathbf{n}) + W_{i+1}^<(\mathbf{n})]\delta_{n_i'}^{1-n_i}\delta_{n_{i+1}'}^{1-n_{i+1}} \prod_{l \neq i,i+1} \delta_{n_l'}^{n_l}, \quad (7)$$

where the probabilities to hop to the right from site i to $i+1$ and to the left from site $i+1$ to i are given, respectively, by

$$W_i^>(\mathbf{n}) = J_0 n_i (1-n_{i+1})[1 + A_1 n_{i-1} + B_1 n_{i+2} + C_{11} n_{i-1} n_{i+2}], \quad (8)$$

$$W_{i+1}^<(\mathbf{n}) = J_0 (1-n_i) n_{i+1}[1 + A_1 n_{i+2} + B_1 n_{i-1} + C_{11} n_{i-1} n_{i+2}]. \quad (9)$$

These general forms express the effect on the transition probabilities due to nearest neighbor interactions (for the present). They can also be written in terms of the occupation configurations of all neighboring sites, e.g.,

$$W_i^>(\mathbf{n}) = J_0 n_i (1-n_{i+1})[(1-n_{i-1})(1-n_{i+2}) + (1+A_1)n_{i-1}$$
$$\times (1-n_{i+2}) + (1+B_1)(1-n_{i-1})n_{i+2} + (1+A_1+B_1$$
$$+ C_{11})n_{i-1}n_{i+2}] \quad (10)$$

with a similar expression for $W_{i+1}^<(\mathbf{n})$. This form is illustrated in Fig. 1. The first term in (10) represents the hopping of a particle which is isolated before and after the jump, with a rate J_0; the second term represents the separation of a particle from a neighbor with a rate $J_0(1+A_1)$; the particle has no neighbors after the event; the third term represents the converse of the process, with a rate $J_0(1+B_1)$. The last term represents the exchange of a particle between blocks. The elementary hopping rate, J_0, usually has a thermally activated form.

Detailed balance puts one condition on the three coefficients, namely,

$$1 + A_1 = (1 + B_1)e^{\beta V_1}. \quad (11)$$

Judicious choices of these coefficients allow us to describe different hopping scenarios that we will discuss below; various choices have been made in the literature.[1,19] For example, if particle-hole symmetry is to be preserved in the

hopping process then the first and fourth terms in Eq. (10) must be the same, which requires that

$$A_1 + B_1 + C_{11} = 0. \tag{12}$$

III. EQUATION OF MOTION AND FICK'S LAW

Taking the first moment of the master equation, i.e., multiplying Eq. (3) by n_i and summing over all microstates **n**, we obtain the equation of motion for the average occupancy of a site. To write this efficiently we introduce a particle current through the bond $i \rightarrow i+1$

$$j_i = a[W_i^>(\mathbf{n}) - W_{i+1}^<(\mathbf{n})] \tag{13}$$

and its average

$$\langle j_i \rangle = a \sum_{\mathbf{n}} [\langle W_i^>(\mathbf{n}) \rangle - \langle W_{i+1}^<(\mathbf{n}) \rangle] = aJ_0[\langle \overrightarrow{\bullet_i \circ_{i+1}} \rangle - \langle \overleftarrow{\circ_i \bullet_{i+1}} \rangle]$$

$$+ A_1(\langle \bullet_{i-1} \bullet_i \circ_{i+1} \rangle - \langle \circ_i \bullet_{i+1} \bullet_{i+2} \rangle) + B_1(\langle \bullet_i \circ_{i+1} \bullet_{i+2} \rangle$$

$$- \langle \bullet_{i-1} \circ_i \bullet_{i+1} \rangle) + C_{11}(\langle \bullet_{i-1} \bullet_i \circ_{i+1} \bullet_{i+2} \rangle - \langle \bullet_{i-1} \circ_i \bullet_{i+1} \bullet_{i+2} \rangle)]. \tag{14}$$

(The arrows indicate the directions of the hops for the two contributions.) Averages are defined by, as examples,

$$\langle \bullet_i \rangle = \langle n_i \rangle(t) = \sum_{\mathbf{n}} n_i P(\mathbf{n},t), \tag{15}$$

$$\langle \bullet_i \circ_{i+1} \rangle = \langle n_i(1-n_{i+1}) \rangle(t) = \sum_{\mathbf{n}} n_i(1-n_{i+1}) P(\mathbf{n},t). \tag{16}$$

The equation of motion then reads

$$\frac{d\langle n_i \rangle}{dt} = \frac{1}{a}[\langle j_{i-1} \rangle - \langle j_i \rangle]. \tag{17}$$

The diffusion equation emerges from this in the long-time and long-wavelength limit for which we can introduce a local density or coverage $\theta(x=ia,t) = \langle n_i \rangle(t)$ and a local current $j(x,t)$. For the latter we get from Eq. (14)

$$j(x,t) = aJ_0\{\theta(x,t) - \theta(x+a,t) + A_1[F_2(x-a,t) - F_2(x+a,t)]$$

$$- A_1[F_3(x,t) - F_3(x+a,t)] + B_1[F_{3h}(x+a,t)$$

$$- F_{3h}(x,t)] + C_{11}[F_{4h}^<(x+a,t) - F_{4h}^>(x,t)]\} \tag{18}$$

in terms of correlation functions with a continuous space and time dependence

$$F_2(x,t) = \langle n_i n_{i+1} \rangle(t),$$

$$F_3(x,t) = \langle n_{i-1} n_i n_{i+1} \rangle(t),$$

$$F_{3h}(x,t) = \langle n_{i-1}(1-n_i) n_{i+1} \rangle(t),$$

$$F_{4h}^<(x,t) = \langle n_{i-2} n_{i-1}(1-n_i) n_{i+1} \rangle(t),$$

$$F_{4h}^>(x,t) = \langle n_{i-1}(1-n_i) n_{i+1} n_{i+2} \rangle(t). \tag{19}$$

For densities varying slowly on the length scale of the lattice constant, i.e., in the continuum limit, we expand the current keeping terms linear in the spatial gradient

$$j(x,t) \approx -a^2 J_0 \left\{ \frac{\partial}{\partial x}[\theta + 2A_1 F_2 - A_1 F_3 - B_1 F_{3h} - C_{11} F_{4h}^<(x)] \right.$$

$$\left. - a^{-1} C_{11}[F_{4h}^<(x) - F_{4h}^>(x)] \right\}. \tag{20}$$

In addition, for long time and length scales, a system is maintained in local equilibrium by much faster relaxation processes. In particular, this implies that the space and time dependence of correlation functions is completely given by that of the local density, i.e., for their gradients we must have

$$\frac{\partial}{\partial x} F_\alpha(x,t) = \frac{d}{d\theta} F_\alpha[\theta(x,t)] \frac{\partial \theta}{\partial x} \tag{21}$$

and we obtain Fick's first law for the diffusion current

$$j(x,t) = -D(\theta) \frac{\partial \theta}{\partial x} \tag{22}$$

with the density-dependent diffusion coefficient

$$D(\theta) = D_0 \left\{ 1 + \frac{d}{d\theta}[A_1(2F_2 - F_3) - B_1 F_{3h}] \right.$$

$$\left. + C_{11} F_{4h} \frac{d}{d\theta} \ln \frac{F_4}{F_{4h}} \right\} \tag{23}$$

in terms of the equilibrium correlators at the local density. Here $D_0 = a^2 J_0$ is the diffusion coefficient in the absence of lateral interactions. We have evaluated the contribution from the last term in Eq. (20) by using the fact that the correlators are those of local equilibrium and hence they factorize exactly, in one-site overlap, for a 1D system with nearest neighbor interactions. Thus we have

$$F_{4h}^<(x) - F_{4h}^>(x) = \langle n_{i-2} n_{i-1}(1-n_i) n_{i+1} \rangle - \langle n_{i-1}(1-n_i) n_{i+1} n_{i+2} \rangle \tag{24}$$

$$= \frac{\langle n_{i-2} n_{i-1} \rangle \langle n_{i-1}(1-n_i) n_{i+1} \rangle}{\langle n_{i-1} \rangle} - \frac{\langle n_{i-1}(1-n_i) n_{i+1} \rangle \langle n_{i+1} n_{i+2} \rangle}{\langle n_{i+1} \rangle} \tag{25}$$

$$= -a \frac{F_{3h}(x)}{\theta(x)} \left[3 \frac{\partial F_2}{\partial x} - 2 \frac{F_2}{\theta} \frac{\partial \theta}{\partial x} \right] + O(a^2) \tag{26}$$

$$= -a \frac{d}{d\theta} \ln \frac{F_2^3}{\theta^2} \frac{\partial \theta}{\partial x} = -a \frac{d}{d\theta} \ln(F_4) \frac{\partial \theta}{\partial x} \tag{27}$$

to first order in a. Combined with the contribution from the first C_{11} term in Eq. (20) this gives the result in Eq. (23).

The fact that for a 1D system all equilibrium correlation functions factorize allows one to write an analytical expression for the coverage dependence of the diffusion coefficient. For nearest neighbor interactions, factorization gives[30]

$$F_2[\theta(x)] = \langle \bullet \bullet \rangle = \langle \bullet \rangle \left[1 - 2 \frac{1-\theta}{1+\alpha} \right], \tag{28}$$

$$\alpha^2 = 1 - 4\theta(1-\theta)(1 - \exp[-\beta V_1]), \tag{29}$$

$$F_3(\theta) = \langle \bullet \bullet \bullet \rangle = \frac{\langle \bullet \bullet \rangle^2}{\langle \bullet \rangle}, \tag{30}$$

$$F_{3h}(\theta) = \langle \bullet \circ \bullet \rangle = \frac{\langle \circ \bullet \rangle^2}{\langle \circ \rangle}. \tag{31}$$

With these expressions the diffusion coefficient becomes, after simplification,

$$D(\theta) = D_0 \frac{(1-r)}{\alpha} \{ 1 + A_1 r + (1-r)\theta[A_1 + B_1 + C_{11}$$
$$\times (\theta + (1-\theta)r)] \}, $$

$$r = \frac{\alpha - 1}{\alpha + 1}. \tag{32}$$

If we set $C_{11}=0$ here we recover Zwerger's result,[9] effectively.

The factorization is also behind the fact that the diffusivity can be expressed as a product of the susceptibilitiy and the average hopping rate, i.e., the Reed-Ehrlich form. We now show this form is rigorously valid for a 1D system with nearest neighbor interactions, i.e., we want to rewrite Eq. (23), here in diagrammatic form,

$$D(\theta) = D_0 \left\{ 1 + \frac{d}{d\theta} [A_1 \langle \bullet \bullet \rangle + A_1 \langle \bullet \bullet \circ \rangle - B_1 \langle \bullet \circ \bullet \rangle] \right.$$
$$\left. + C_{11} \langle \bullet \bullet \circ \bullet \rangle \frac{d}{d\theta} \ln \frac{\langle \bullet \bullet \bullet \bullet \rangle}{\langle \bullet \bullet \circ \bullet \rangle} \right\}, \tag{33}$$

$$= \frac{1}{2} a^2 \chi^{-1} \langle W_i^>(\mathbf{n}) + W_{i+1}^<(\mathbf{n}) \rangle, \tag{34}$$

$$= D_0 \chi^{-1} [\langle \bullet \circ \rangle + A_1 \langle \bullet \bullet \circ \rangle + B_1 \langle \bullet \circ \bullet \rangle + C_{11} \langle \bullet \bullet \circ \bullet \rangle], \tag{35}$$

where

$$\chi^{-1} = \left. \frac{\partial \beta \mu}{\partial \theta} \right|_T = [\alpha \theta (1 - \theta)]^{-1} \tag{36}$$

is the inverse susceptibility, given as a derivative of the chemical potential

$$\exp[\beta \mu] = \frac{\alpha - 1 + 2\theta}{\alpha + 1 - 2\theta} \exp[\beta V_1].$$

To show that Eqs. (33) and (35) are equal we first eliminate B_1 in favor of A_1 by using detailed balance Eq. (11). In this new expression A_1 and C_{11} are arbitrary functions of temperature alone, to be chosen independently of each other according to the kinetics envisaged. Thus the terms multiplying them must be equal on either side, e.g., for the terms independent of A_1 and C_{11} we must have

$$1 + (1 - e^{-\beta V_1}) \frac{d}{d\theta} \langle \bullet \circ \bullet \rangle = \langle \bullet \circ \rangle \chi^{-1}. \tag{37}$$

This can be shown by direct differentiation. A more involved identity follows from the terms proportional to A_1. As for the

C_{11} term this is almost trivial because (Appendix B)

$$\frac{\langle \bullet \bullet \bullet \bullet \rangle}{\langle \bullet \bullet \circ \bullet \rangle} = \frac{\langle \bullet \bullet \bullet \rangle}{\langle \bullet \circ \bullet \rangle} = \exp[\beta \mu - 2\beta V_1] \tag{38}$$

with further forms given after factorization into two-site correlators and with use of the identity

$$\langle \bullet \bullet \rangle \langle \circ \circ \rangle = e^{-\beta V_1} \langle \bullet \circ \rangle^2. \tag{39}$$

IV. RESULTS FOR NEAREST NEIGHBOR INTERACTIONS ONLY

In this section we will give explicit results for various choices of diffusion kinetics, namely initial state interactions ($B_1=C_{11}=0$), final state interactions ($A_1=C_{11}=0$), symmetric (initial and final state) interactions ($A_1=-B_1, C_{11}=0$); we compare these with cases where C_{11} is chosen nonzero. Table I summarizes various limiting behaviors of the diffusivity, discussed below, in the cases of strong nearest neighbor repulsion or attraction which follow from these choices.

A. Initial state interactions

In this scenario one assumes that only the initial neighborhood of the hopping particle is important, i.e., that the hopping probability is not influenced by the final environment, and is the one encountered frequently in the literature. In the picture of transition state theory this corresponds to the situation where the accommodation coefficient is unity, namely, that the particle will complete the hop once it is on top of the diffusion barrier between the sites. With $B_1=0$ detailed balance gives

$$A_1 = e^{\beta V_1} - 1. \tag{40}$$

Consistent with this scenario, we choose $C_{11}=0$.

In Fig. 2(a) we show the behaviour with coverage of the diffusivity and the average hopping rate, both normalized to the values for a noninteracting system, for several values of βV_1. For sufficiently large repulsion and attraction we obtain the analytic forms of D shown in Table I, for this case, by using the limiting forms of α. In particular, for large repulsion and $\theta < 1/2$, $\alpha \to +(1-2\theta)$ and $D/D_0 \to (1-2\theta)^{-2}$, while for $\theta > 1/2$, $\alpha \to -(1-2\theta)$ and $D/D_0 \to A_1 \theta^{-2}$. Thus diffusion is accelerated above 1/2 ML, exponentially in the interaction strength. If one performs an Arrhenius analysis of D, i.e., by assigning

$$D/D_0 = \nu \exp(-\beta E_b) \tag{41}$$

and determining the prefactor ν and the diffusion barrier E_b (relative to that of an isolated particle), one finds a barrier stepping down from its value at low coverage, by $-V_1$, around 1/2 ML. The coverage variation of the barrier and prefactor for this case appear elsewhere.[10] For sufficiently strong attraction $\alpha \to [\theta(1-\theta)]^{1/2} \exp(-\beta V_1/2)$, $D/D_0 \to (1-\theta)/2\alpha^3$ and the diffusion decreases rapidly with the interaction strength.

B. Final state interactions

In this scenario the final neighborhood of the hopping particle is relevant. We set $A_1=0$ and get

TABLE I. Limiting forms of the diffusivities for different kinetics and extreme repulsion and attraction between nearest neighbors.

Kinetics	A_1	B_1	C_{11}	$\beta V_1 \to \infty$	$\beta V_1 \to -\infty$
initial state	$e^{\beta V_1}-1$	0	0	$(1-2\theta)^{-2}, \theta<1/2$ $\theta^{-2}e^{\beta V_1}, \theta>1/2$	$\frac{1}{2}(1-\theta)[\theta(1-\theta)]^{-3/2}e^{3\beta V_1/2}$
			$-A_1$	$(1-2\theta)^{-1}(1-\theta)^{-2}$	$\frac{1}{2}[\theta(1-\theta)]^{-3/2}e^{3\beta V_1/2}$
final state	0	$e^{-\beta V_1}-1$	0	$(1-\theta)^{-2}, \theta<1/2$ $(2\theta-1)^{-1}e^{-\beta V_1}, \theta>1/2$	$\frac{1}{2}\theta[\theta(1-\theta)]^{-3/2}e^{\beta V_1/2}$
			$-B_1$	$(1-\theta)^{-2}$	$\frac{1}{2}[\theta(1-\theta)]^{-1}e^{\beta V_1}$
p-h symmetry	$\tanh(\beta V_1/2)$	$-A_1$	0	$(1-\theta)^{-2}$	$\frac{1}{2}[\theta(1-\theta)]^{-3/2}e^{3\beta V_1/2}$
p-h asymmetry	$\tanh(\beta V_1/2)$	$-A_1$	$-A_1$	$(1-\theta)^{-2}, \theta<1/2$ $(2\theta-1)^{-1}e^{-\beta V_1}, \theta>1/2$	$\frac{1}{2}\theta[\theta(1-\theta)]^{-3/2}e^{\beta V_1/2}$
			$-B_1$	$(1-\theta)^{-2}, \theta<1/2$ $2\theta^{-2}, \theta>1/2$	

$$B_1 = e^{-\beta V_1} - 1. \tag{42}$$

Again, we choose $C_{11}=0$, to ensure that the initial neighborhood is irrelevant. Figure 2(b) shows the coverage dependence of D and $\langle W \rangle$, for the same parameters as Fig. 2(a). The effects of this choice of kinetics on the diffusivity are just the opposite to those for the case above. Thus, above 1/2 ML, D decreases below $D(\theta=0)$ for any moderate repulsion while it must eventually increase above $D(0)$ for moderate attraction. [If the ordinate of Fig. 2(b) is set to a logarithmic scale then a transposition of the curves of Fig. 2(a) about 1/2 ML is produced, with appropriate shifting along the ordinate.] In particular, for sufficiently strong repulsion the system behaves as one with nearest neighbor exclusion, i.e., the (empty) site to which the particle is hopping cannot have an occupied neighbor. Consequently, $\langle W \rangle$ must decrease with increasing coverage and vanish as $\theta \to 1/2$; because χ^{-1} is

diverging in the vicinity of this point D rises, instead, and then decreases abruptly above 1/2 ML. One finds $D/D_0 \to (1-\theta)^{-2}$ for $\theta<1/2$, i.e., finite at 1/2 ML.

C. Initial and final state interactions

We treat several scenarios under this heading. First, we extend the above two cases by allowing C_{11} to be finite. An obvious physical choice is to specify particle-hole symmetry for the diffusivity in addition to the above constraints.

Case I: $A_1=-C_{11}=e^{\beta V_1}-1$, $B_1=0$. Figure 2(c) exhibits this particle-hole symmetry in $D(\theta)$, with a logarithmic scale similar to Fig. 2(a). For strong repulsion D diverges around 1/2 ML as $(1-2\theta)^{-1}(1-\theta)^{-2}$. The symmetric increase and decrease of D about 1/2 ML for $V_1>0$ follows from that of $\langle W \rangle$: its form in Eq. (35) becomes $[\langle \bullet \circ \rangle + A_1 \langle \bullet \bullet \circ \circ \rangle]$ so that hopping is accelerated by the interaction in the initial con-
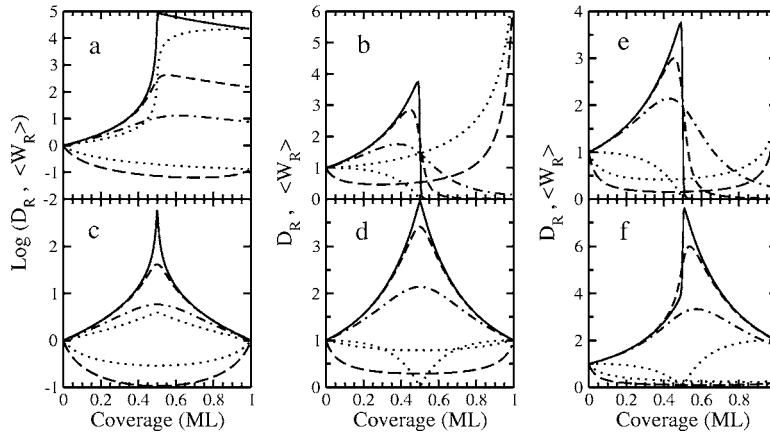

FIG. 2. The coverage dependence of the diffusivity, D, and the average hopping rate $\langle W \rangle$ for varying first neighbor interaction strength and hopping kinetics; each displayed relative to its value for a noninteracting adsorbate $D_R=D/D_0$, $(D_0=J_0a^2)$, $\langle W_R \rangle=\langle W \rangle/\langle W_0 \rangle$, $[\langle W_0 \rangle =J_0\theta(1-\theta)]$. D_R is shown for $V_1=1000k_B$ K, $T=100$ K (solid line), $T=200$ K (dash), $T=500$ K (dash-dot), and $V_1=-1000k_B$ K, $T=200$ K (long dash); $\langle W_R \rangle$ (dotted line) is shown for the extreme repulsion and attraction only. Hopping kinetics: initial state interactions only, $A_1=e^{\beta V_1}-1$, panel (a); final state interactions only, $B_1=e^{-\beta V_1}-1$, panel (b); initial and final state interactions with $C_{11}=-A_1$, panel (c), $C_{11}=-B_1$, panel (d); initial and final state interactions with $A_1=-B_1=\tanh(\beta V_1/2)$ and $C_{11}=-A_1$, panel (e), $C_{11}=-B_1$, panel (f).

figuration $(A_1 > 1)$ provided the neighboring site of the final state is also empty; the probability of this final state configuration $\langle \bullet \circ \bullet \circ \rangle$ is a maximum at $\theta = 1/2$ and decreases steadily thereafter. For initial-state attraction, on the other hand, the pertinent correlators for Figs. 2(a) and 2(c) are similar, $\langle \bullet \bullet \circ \rangle \simeq \langle \bullet \bullet \circ \circ \rangle$, except as monolayer coverage is approached and the magnitude of D is similar as a result.

Case II: $B_1 = -C_{11} = e^{-\beta V_1} - 1, A_1 = 0$. For sufficiently strong interactions the resulting curves for D and $\langle W \rangle$ in Fig. 2(d). are the same as those in Fig. 2(b) for $\theta < 1/2$ and the reflections of these for $\theta > 1/2$. Again this symmetry arises from the correlator combination in $\langle W \rangle$, which can be written as $[\langle \bullet \circ \rangle - (1 - e^{-\beta V_1})\langle \circ \bullet \circ \bullet \rangle]$; the second correlator is again that of case I but it now specifies the configuration of the initial state.

Next we consider cases where both the initial and final states fully influence the kinetics, e.g., with particle repulsion, a neighbor to the hopping particle in its initial configuration aids the hop while a neighbor in the final configuration hinders it. This is achieved by setting $A_1 = -\gamma B_1$ where γ is a parameter of order unity; we have a symmetric influence with $\gamma = 1$, a choice also made by Dieterich *et al.*[1] and Zwerger.[9] We illustrate D and $\langle W \rangle$ for three choices of C_{11} made already.

Case III: $A_1 = -B_1 = \tanh(\beta V_1/2), C_{11} = 0$. This case was discussed originally by Zwerger and gives rise to a particle-hole-symmetric diffusivity. Its coverage dependence is similar to that of Fig. 2(d) and identical in the limit of strong repulsion; for strong attraction the limiting value differs, see Table I.

Case IV: $A_1 = -B_1 = \tanh(\beta V_1/2), C_{11} = -A_1$ [Fig. 2(e)]. The particle-hole symmetry is maximally broken with $D(\theta = 1)/D_0 = 1 + C_{11}$. For particle repulsion the coverage dependence of D is nearly identical to that of Fig. 2(b). For strong repulsion $(A_1 \to 1)$ it is easy to see why $- \langle W \rangle J_0^{-1} \to \langle \bullet \circ \circ \rangle + \langle \bullet \bullet \circ \circ \rangle \simeq \langle \bullet \circ \circ \rangle$ for all θ.

Case V: $A_1 = -B_1 = \tanh(\beta V_1/2), C_{11} = -B_1$ [Fig. 2(f)]. For repulsive interactions the peak value of D is about twice as large as the previous cases. Again, $D(1)/D_0 = 1 + C_{11}$.

V. DIFFUSION BEYOND FIRST NEIGHBOR INTERACTIONS

A. Diffusivity

We now generalize our approach to include second nearest neighbor (V_2) and trio (V_t) interactions between particles. The general forms of the transition probabilities Eqs. (8) and (9) now expand to sixteen terms each, for example,

$$W_i^>(\mathbf{n}) = J_0\{n_i(1 - n_{i+1})[1 + n_{i-1}(A_1 + n_{i-2}(A_{11} + A_{111}n_{i+2}))$$
$$+ n_{i-2}(1 - n_{i-1})(A_{10} + A_{101}n_{i+2}) + A_{1101}n_{i-2}n_{i-1}$$
$$\times (1 - n_{i+2})n_{i+3} + ((B_{111}n_{i-1} + B_{11})n_{i+3} + B_1)n_{i+2}$$
$$+ (B_{101}n_{i-1} + B_{10})(1 - n_{i+2})n_{i+3} + B_{1101}n_{i-2}$$
$$\times (1 - n_{i-1})n_{i+2}n_{i+3} + C_{11}n_{i-1}n_{i+2} + n_{i-2}n_{i+3}$$
$$\times (C_{1001}(1 - n_{i-1})(1 - n_{i+2}) + C_{1111}n_{i-1}n_{i+2})]\} \quad (43)$$

with a similar expression for $W_{i+1}^<(\mathbf{n})$. The labels of the coefficients here specify the occupations of the neighborhood of the pair of sites exchanging the particle. The A and B coefficients are related by detailed balance; there are now three C coefficients as free parameters which attend the completely symmetric neighborhood. Some details about the relations between these parameters and their values for some choices of kinetics are gathered in Appendix A. We calculate the average current through a bond and convert this to a local current $j(x,t)$ by introducing additional time and space-dependent correlators, ranging up to six sites. The majority of these are asymmetric with respect to a reflection about their midpoint; we distinguish these asymmetric pairs by superscripts $(>, <)$, see $F_{4h}^>, F_{4h}^<$, and list one member of each pair, only, obtaining the other by replacing the indices $i+a$ by $i-a$ for $a = 1, 2, 3$:

$$F_4(x) = \langle n_{i-1}n_i n_{i+1}n_{i+2} \rangle,$$

$$F_{42h}(x) = \langle n_{i-1}(1 - n_i)(1 - n_{i+1})n_{i+2} \rangle,$$

$$F_{5h1}(x) = \langle n_{i-2}n_{i-1}(1 - n_i)n_{i+1}n_{i+2} \rangle,$$

$$F_{5h}^<(x) = \langle n_{i-2}n_{i-1}n_i(1 - n_{i+1})n_{i+2} \rangle,$$

$$F_{52h}^<(x) = \langle n_{i-2}n_{i-1}(1 - n_i)(1 - n_{i+1})n_{i+2} \rangle,$$

$$F_{5h2}(x) = \langle n_{i-2}(1 - n_{i-1})n_i(1 - n_{i+1})n_{i+2} \rangle,$$

$$F_{6h}^<(x) = \langle n_{i-3}n_{i-2}n_{i-1}(1 - n_i)n_{i+1}n_{i+2} \rangle,$$

$$F_{62h}^<(x) = \langle n_{i-3}n_{i-2}n_{i-1}(1 - n_i)(1 - n_{i+1})n_{i+2} \rangle,$$

$$F_{6h2}^<(x) = \langle n_{i-3}n_{i-2}(1 - n_{i-1})n_i(1 - n_{i+1})n_{i+2} \rangle,$$

$$F_{63h}^<(x) = \langle n_{i-3}(1 - n_{i-2})n_{i-1}(1 - n_i)(1 - n_{i+1})n_{i+2} \rangle. \quad (44)$$

The expansion of $j(x,t)$ in the spatial gradient gives terms with the general form of Eq. (20), namely, direct spatial derivatives of combinations of all correlators and differences of all pairs of asymmetric correlators. These differences can be evaluated by factorization of the correlators but now in two-site overlap, as this is exact for interactions over two lattice sites for a 1D system in local equilibrium. For example, in place of Eq. (25) we have

$$F_{4h}^<(x) - F_{4h}^>(x) = \frac{\langle n_{i-2}n_{i-1}(1 - n_i) \rangle \langle n_{i-1}(1 - n_i)n_{i+1} \rangle}{\langle n_{i-1}(1 - n_i) \rangle}$$
$$- \frac{\langle n_{i-1}(1 - n_i)n_{i+1} \rangle \langle (1 - n_i)n_{i+1}n_{i+2} \rangle}{\langle (1 - n_i)n_{i+1} \rangle}$$

$$(45)$$

$$= -a \frac{F_{3h}}{(\theta - F_2)} \left[3\frac{\partial F_2}{\partial x} - 2\frac{\partial F_3}{\partial x} - \left(2\frac{\partial \theta}{\partial x} - \frac{\partial F_2}{\partial x}\right) \frac{(F_2 - F_3)}{(\theta - F_2)} \right]$$

$$(46)$$

$$=-aG_{4h}(\theta)\frac{\partial\theta}{\partial x} \qquad (47)$$

which defines a function of the local density $G_{4h}[\theta(x),t]$ analogous to Eq. (27). Because the parent correlator, $F_{4h}(x) = F_{3h}(F_2-F_3)/(\theta-F_2)$, can be factored from this expression we may also write

$$G_{4h}(\theta)=F_{4h}\left[\frac{1}{(F_2-F_3)}\frac{d}{d\theta}(3F_2-2F_3)\right.$$
$$\left.-\frac{1}{(\theta-F_2)}\frac{d}{d\theta}(2\theta-F_2)\right], \qquad (48)$$

$$=F_{4h}H_{4h}. \qquad (49)$$

All asymmetric differences can be written in this manner. The final expression for the diffusivity is

$$D(\theta)/D_0 = 1 + 2A_1F_2' + (3A_{11}-A_1)F_3' + (3A_{10}-B_1)F_{3h}'$$
$$-2A_{11}F_4'-2B_{10}F_{42h}'+C_{11}(G_{4h}-F_{4h}')+A_{10}$$
$$\times(G_{4h}-3F_{4h}')-B_{11}(G_{4h}+F_{4h}')+A_{111}(G_{5h}+F_{5h}')$$
$$-B_{111}F_{5h1}'+A_{101}F_{5h2}'+B_{101}(G_{52h}-F_{52h}')$$
$$+C_{1111}(G_{6h}-F_{6h}')+A_{1101}(G_{62h}-F_{62h}')$$
$$-B_{1011}(G_{6h2}-F_{6h2}')+C_{1001}(G_{63h}-F_{63h}'), \qquad (50)$$

where the prime indicates a derivative of the particular correlator with respect to coverage θ. The functions $H_\alpha = G_\alpha/F_\alpha$ are listed in Appendix B.

Although it is not obvious, this expression *also* transforms to the Reed-Ehrlich product form Eq. (34) for arbitrary values of the kinetic coefficients, provided only that they satisfy detailed balance. The clue that the transformation exists is provided by the multipliers of the free parameters C_{1111}, C_{1001} in Eq. (50). Both of these can be written as a product of χ^{-1} and the corresponding correlator, directly. For example, using (B10) we have,

$$(G_{6h}-F_{6h}')=(F_{6h}H_{6h}-F_{6h}') \qquad (51)$$

$$=-\langle\bullet\bullet\bullet\bullet\bullet\bullet\rangle\frac{d}{d\theta}\ln\frac{\langle\bullet\bullet\bullet\circ\bullet\bullet\rangle}{\langle\bullet\bullet\bullet\bullet\bullet\bullet\rangle}\frac{\partial\theta}{\partial x}. \qquad (52)$$

The quotient here can be factored down to Eq. (B5); χ^{-1} follows. Although we have no analytical proof of the transformation for the remaining terms in Eq. (50), due to the nonlinear relations between correlators, we have shown it to desired numerical precision. As we have employed both linear and nonlinear interactions, by extension, we can expect the product form of the diffusivity to exist for any interactions between particles on a 1D lattice and for the most general forms of the kinetic coefficients.

B. Results

With two additional interactions and many more options for the detailed kinetics of hopping we must select just a few representative cases to illustrate new features and highlight
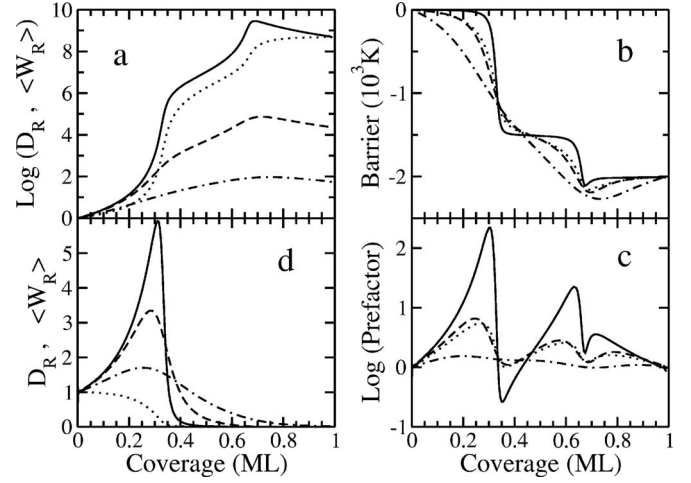

FIG. 3. (a) The coverage dependence of the diffusivity for first and second neighbor repulsions of $V_1=2V_2=1000k_B$ K and temperatures $T=100$ K (solid line), $T=200$ K (dash), $T=500$ K (dash-dot); and the average hopping rate for $T=100$ K (dotted line). Hopping kinetics have initial state interactions. (b) The change of the hopping barrier E_b with coverage obtained from a differential, isosteric Arrhenius analysis of the diffusivity in panel (a), for the same temperatures; the standard linear fit through the isosteres (temperature average) is shown as a dotted line. (c) Corresponding prefactor ν. (d) As panel (a) but with the kinetics of final state interactions.

the intricate interplay between the effects of interactions and kinetics. To contain the number of examples we note that if all interactions sum up to a net attraction then, typically, the coverage dependence of the diffusivity is similar to that illustrated in Fig. 2 for attractive nearest neighbor interaction only; we shall not consider such cases again.

For a typical chemisorption system, such as CO on transition or noble metals, the first neighbor interaction is strongly repulsive and weaker further neighbor interactions can be either attractive or repulsive. These cases are exemplified in the figures below where we choose the same range for V_1/k_BT as in Fig. 2.

In Fig. 3(a) we have initial state interactions only (the seven nonzero kinetic coefficients are given in Appendix A), as the extension of Fig. 2(a). For a weaker second neighbor repulsion two ordered structures occur, namely, at coverages 1/3 and 2/3 ML, which give rise to two peaks in the inverse susceptibility (see Fig. 4) and two corresponding steep rises in the diffusivity; these are washed out as temperature is increased. A clearer picture of the underlying energetics emerges from an Arrhenius analysis of several isotherms of D/D_0, spanning low to moderate temperatures. The barrier, E_b, clearly exhibits the effect of the neighbors on the hopping particle [Fig. 3(b)]. At low temperature and at coverage 1/3 (plus one particle) the structure around the hopping particle (∗) is •∘∘•∗∘•∘∘•, i.e. it interacts with one first and one second neighbor initially, escaping both after the jump. Thus around 1/3 ML the activation barrier is reduced by V_1+V_2. Similarly, at 2/3 ML, the equilibrium structure has 2 of every 3 neighboring sites occupied and the hopping particle sees an additional second neighbor initially. Correspondingly the barrier is reduced by V_2 above this coverage.
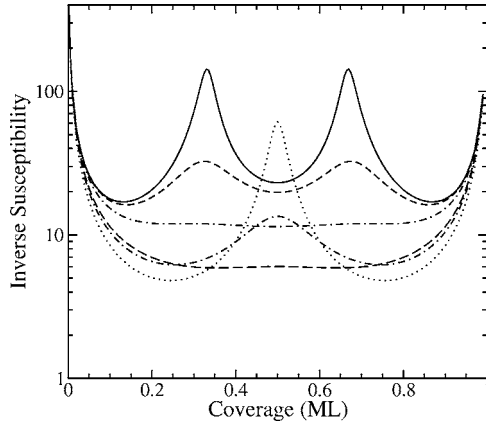
FIG. 4. Dependence of the inverse susceptibility of a 1D adsorbate on coverage and temperature for two interaction sets, (i) $V_1 = 2V_2 = 1000k_B$ K (upper 3 lines at 1/3 ML), $T=100$ K (solid), $T=200$ K (dash), $T=500$ K (dash-dot), and (ii) $V_1 = -2V_2 = 1000k_B$ K, $T=300$ K (dotted), $T=500$ K (dash-dot), $T=1000$ K (long dash).

The prefactor, v, being a measure of the order (change in entropy) of the adsorbate shows minima at these coverages [Fig. 3(c)]. For final state interactions alone, all effects and results are essentially the converse of the above, Fig. 3(d). Thus, for strong repulsion, D/D_0 initially rises for $\theta < 1/3$, as $(1-2\theta)^{-2}$; this is purely an entropic effect arising from first and second neighbor exclusion, there being no energy cost to hop below 1/3 ML. Above this coverage D/D_0 drops by $\exp(-\beta V_2)$ as the hopping particle sees a second neighbor when in its final state; at 2/3 ML, it plummets again, by $\exp(-\beta[V_1+V_2])$, due to the second well-ordered neighborhood. An Arrhenius analysis produces the reflections of Figs. 3(b) and 3(c) (about $\theta=1/2$ and $E_b=0$).

Next we consider some cases of initial and final state interactions. Among the many choices available for the kinetics we shall follow cases III–V in the previous section, with the generalisation of the condition $A_1 = -B_1$ to all such pairs, $A_{mn...} = -B_{nm...}$ (see Appendix A), and three sets of the remaining parameters: $C_{1001} = C_{1111} = 0$, and $C_{11} = 0$ (case VI), $C_{11} = -A_1$ (case VII), $C_{11} = -B_1$ (case VIII).

Case VI [Fig. 5(a)]. D is symmetric about 1/2 ML for this choice of the kinetic coefficients, see Eq. (A9). For low enough temperature the effect of the ordering of the adsorbate on the diffusivity for $\theta < 1/3$ has a similar result to that of final state interactions. However a hopping particle experiences no energy change as a result of its jump for $1/3 < \theta < 1/2$ and the average hopping rate $\langle W \rangle$ while passing through a minimum at 1/3 ML, does not change significantly, with the result that D does not diminish much, either, in this region. This is confirmed by a differential Arrhenius analysis which shows, again, that the variation of D at lowest temperatures is due to entropy changes alone. [Note that a standard analysis, a straight line fitted to isosteres of $\ln(D)$ vs $1/T$, gives a misleading account of the prefactor because the isosteres are curved for this example at high temperature.]

Case VII. [Fig. 5(b)]. Here $\langle W \rangle$, hence D, decreases exponentially with interaction strength above 2/3 ML for low temperature. This case is the counterpart to Fig. 2(e) and a
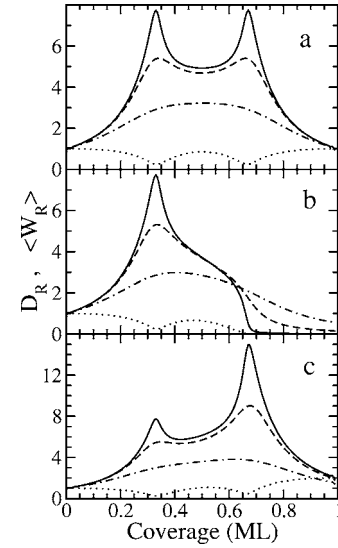

FIG. 5. The diffusivity and average hopping rate for the interactions and temperatures of Fig. 3 and for the hopping kinetics of initial and final state interactions varying: $A_{mn...} = -B_{nm...}$, $C_{1001} = C_{1111} = 0$, and $C_{11} = 0$ [panel (a)], $C_{11} = -A_1$ [panel (b)], $C_{11} = -B_1$ [panel (c)].

similar analysis of the contributions to $\langle W \rangle$ explains the decrease: The symmetry-breaking term $C_{11}\langle \bullet\bullet\circ\bullet \rangle$ subtracts from $A_1\langle \bullet\bullet\circ \rangle$ to give $A_1\langle \bullet\bullet\circ\circ \rangle$ (with $A_1 = \tanh(\beta[V_1-V_2]/2)$ now); this correlator diminishes above 1/2 ML and rapidly above 2/3 ML. An Arrhenius analysis confirms a barrier of (V_1-V_2) at 2/3 ML.

Case VIII. [Fig. 5(c)]. Because the symmetry-breaking factor only adds the term $A_1\langle \bullet\bullet\circ\bullet \rangle$ to the expression for $\langle W \rangle$ in case VII, the average hopping rate and D can increase modestly, only, above 2/3 ML; compare the first-neighbor-only counterpart, Fig. 2(f).

These three cases show that the coverage variation of the diffusivity is noticeably affected by the variation in just one of several kinetic coefficients; variations of C_{1001} or C_{1111} produce different results again. In Fig. 6 we present a few results for other interactions. In panels (a), (b) we have changed the sign of V_2 to have attraction between second neighbors. There is only one ordered structure because, at low temperature, nearest neighbor sites are not occupied until coverage 1/2 is reached. Here the chemical potential rises by $2V_1$ and the inverse susceptibility exhibits a sharp peak, with deep minima at 1/4, 3/4 ML associated with the second neighbor attraction (see Fig. 4). This behavior of χ^{-1} is reflected in the diffusivity for temperatures smaller than about V_1/k_B. Figure 6(a) has initial state interactions for the kinetics. Figure 6(b) has the coefficients of case VII (initial and final state interactions with $C_{11} = -A_1$); if $C_{11} = 0$ instead, then D and $\langle W \rangle$ above 1/2 ML would reflect the behavior shown below 1/2 ML in panel (b); for $C_{11} = -B_1$, however, D and $\langle W \rangle$ are not dissimilar to panel (a). In Figs. 6(c) and 6(d) we supplement the interactions of Figs. 3 and 5 with a trio attraction, $V_t = -V_2$. In panel (c) we have again assigned initial state interactions only. Not surprisingly, the effect of this additional attraction is to offset the rise of the diffusivity above 1/3 ML in Fig. 3(a). Conversely, a trio repulsion en-

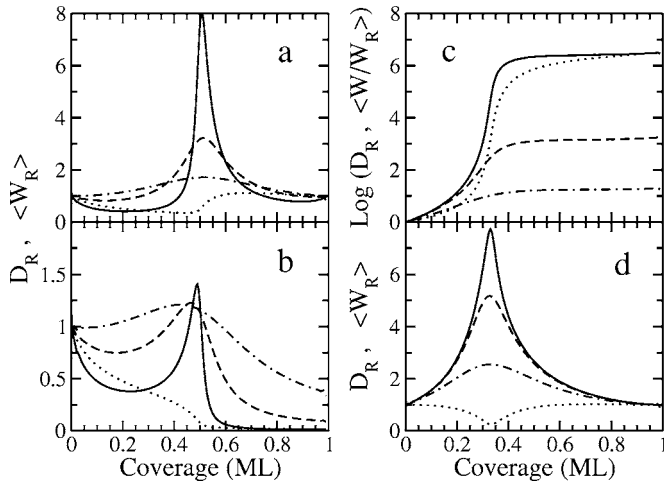FIG. 6. (a),(b) The diffusivity for first neighbor repulsion and second neighbor attractions of $V_1 = -2V_2 = 1000k_B$ K, and temperatures $T = 300$ K (solid line), $T = 500$ K (dash), $T = 1000$ K (dash-dot); and the average hopping rate for $T = 300$ K (dotted line). Hopping kinetics are those of initial state interactions only (a) and case VII (b). (c),(d) Interactions and temperatures of Fig. 3 with a trio attraction added, i.e., $V_1 = 2V_2 = -2V_t = 1000k_B$ K, and initial state interactions only (c) or symmetric initial and final state interactions (d).

hances the rise of D around 2/3 ML by a factor $\exp(\beta V_t)$. In panel (d) the kinetic coefficients are those of Case VI; the trio attraction now suppresses, completely, both the minimum of $\langle W \rangle$ and the peak of D around 2/3 ML in Fig. 5(a).

As a final, but significant, example of the interplay between the interactions and kinetics, we present in Fig. 7 two panels generated with distinct values of both sets of parameters. Panel (a) has the interactions of Fig. 3(d) ($V_1 = 2V_2$
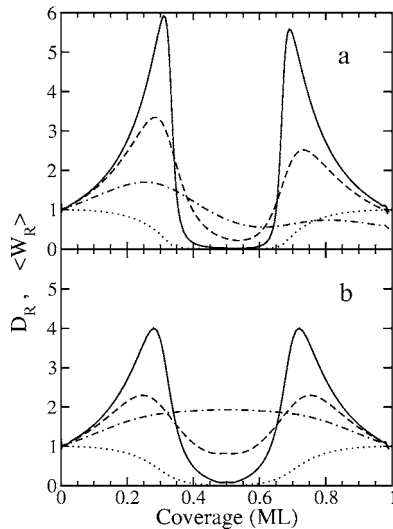

FIG. 7. (a) The diffusivity and average hopping rate for the interactions and temperatures of Fig. 3 ($V_1 = 2V_2 = 1000k_B$ K), and kinetic coefficients assigned those of final state interactions with $C_{11} = C_{1111} = -A_1$ in addition. (b) Interactions of panel (a) interchanged ($2V_1 = V_2 = 1000k_B$ K) and kinetic coefficients those of symmetric initial and final state interactions.

$= 1000k_B$K) and with a modification to the kinetics there by setting $C_{11} = C_{1111} = -A_1$. The nonzero value of C_{1111} introduces just one more initial state into the kinetics. The effect of this choice for the free parameters is to make the diffusivity almost symmetric around 1/2 ML, except at highest temperature. In contrast, panel (b) has this symmetry enforced with the standard choice of initial-and-final state interactions (case VI) but now with the interactions interchanged $V_1 = 1/2V_2 = 500k_B$K. But for an adjustment in scale, the average hopping rates and diffusivities are quite similar in these two panels. Not surprisingly, a standard Arrhenius analysis does not differentiate the interactions in these two cases. Other examples of distinct interaction sets and kinetic parameters producing a similar coverage dependence of the diffusivity exist.

VI. DISCUSSION AND SUMMARY

By applying a gradient expansion of the correlators in the diffusion current of a 1D adsorbate, we have derived analytic expressions for the collective diffusivity as a function of local coverage, valid for all choices of the hopping kinetics and lateral interactions out to second neighbors, including nonlinear (trio) interactions. Also, we have shown that the diffusivity can be expressed as a product of the average hopping rate (a kinetic factor) and the inverse susceptibility (a thermodynamic factor). Underpinning these results is the exact factorization of correlators down as far as $(m+1)$-site quantities, with m-site overlap, for interactions to mth neighbors. Thus the Reed-Ehrlich product form should exist for any range of interactions and for any forms of the kinetic coefficients satisfying detailed balance. Our calculational method is transparent and the more so by employing diagrammatic representations of the correlators where possible.

We have presented numerical examples of the coverage and temperature dependence of the diffusivity for a range of interactions and choices of kinetic coefficients. Of note is the fact that effects of one choice of interactions and kinetics can be mimicked, or nearly so, with a different choice of one or both sets of parameters. Only the case of initial-state interactions for the kinetics with significant particle repulsions stands apart: here the diffusivity increases exponentially with the interaction strength as the coverage increases through that of the ordered structures. For other choices of the kinetics, a unique interpretation of features, such as peaks in the diffusivity, as due to a particular set of interactions is not possible. Thus one needs, first, equilibrium data on a particular adsorbate to extract the interaction parameters before one can attempt to extract the kinetics from the diffusion data. This situation is very much akin to that of interpreting thermal desorption spectra, where it has been demonstrated, repeatedly, that a unique description of a particular adsorbate can only be achieved if a large set of equilibrium and kinetic (adsorption-desorption) data is analyzed.[21]

For the case of first neighbor interaction alone, the various diffusivity results arose in part from the choices of the free parameter C_{11}. In previous work this parameter has been ignored or assumed to vanish, for computational efficacy. In particular, in his examination of diffusivity in 1D using lin-

ear response theory, Zwerger[9] assumed $C_{11}=0$; in a corresponding examination of conductivity in 1D, Singer and Peschel[20] did the same. We repeat their argument: The Green-Kubo expression for the generalised conductivity for a 1D lattice is

$$\sigma(\omega) = \sigma(\infty) - \beta N_s^{-1} \int_0^\infty dt \exp(i\omega t)\langle J(t)J(0)\rangle, \quad (53)$$

$$\sigma(\infty) = \frac{\beta}{2}a^2[\langle W_i^>(\mathbf{n})\rangle + \langle W_{i+1}^<(\mathbf{n})\rangle]. \quad (54)$$

The collective diffusion coefficient is obtained from the dc conductivity and the static structure factor $S(q)$, as $D = \sigma(0)/\theta\beta S(q=0)$, i.e., in the hydrodynamic limit. Here J is the net particle current, in the present case,

$$J = \sum_i j_i = C_{11}\sum_i n_{i-1}(1-n_i)n_{i+1} \quad (55)$$

with the A_1 and B_1 terms summing to zero. Thus, for $C_{11}=0$, the calculation of D simplifies to the evaluation of $\sigma(\infty)$ and $S(0)$ (i.e., χ^{-1}) and the product form of D is guaranteed. No such restriction is necessary in our approach. When interactions to second neighbors are included the number of terms in Eq. (55) increases to nine, these corresponding to all the asymmetric correlators present in $\langle W_i(\mathbf{n})\rangle$. Clearly, the neglect of the second term in Eq. (53) may grossly misrepresent the diffusivity in this case.

We discuss, briefly, other approaches to the analytical calculation of the diffusivity which are applicable to 1D systems. Kikuchi developed the path probability method for diffusion as the nonequilibrium extension of the cluster variation method.[12,13] In the cluster method correlators are also factorized. Applied to a one-dimensional system with nearest neighbor interactions[22] his result has the kinetics of initial state interactions. However, the path probability method is not transparent and relatively complicated to extend to more general cases, including 2D systems, without severe approximations.[23]

Chvoj[14] has developed a similar method to ours, using a Kramers-Moyal expansion of the master equation to introduce a coverage gradient term as a starting point for the evaluation of the diffusivity. He evaluates the latter, for a square lattice, by invoking the quasichemical approximation with first neighbor interaction and initial-state kinetics with saddle-point modifications; the quasichemical approximation is again a factorization result. For strong interaction his results are in contradiction to earlier work based on the Green-Kubo formula.

Recently Gortel et al[10] have calculated the diffusivity of a 1D adsorbate with nearest neighbor interactions using a variational technique to extract the leading eigenvalue of the transition rate matrix in the master equation (3). Their formula for D is equivalent to Eq. (32) upon rearrangement and results are presented for the case of initial-state interactions, only. In a subsequent paper[24] the product form of the diffusivity is realized and long-range nearest neighbor interactions are treated. However, their method is computationally involved, even for the simplest case.

In contrast to the above approaches, extensions of our method in 1D to include more than one binding site, particle jumps longer than one site, or other specific kinetics (e.g., saddle point effects[5,14]), appear to be straightforward. Only the number and complexity of the correlators appearing in Eq. (34) increases. However, their factorization will simplify the results; the latter should again be transparent in interpretation as, for example, in the case of the equilibrium and sticking properties of a two-binding site adsorbate.[25] The method also lends itself to an analysis of diffusion in 2D systems; the work reported here was the precursor to such an analysis. The gradient expansion is now that of correlators in 2D which, assuming factorization, can again be expanded in terms of the local density and functions which can be calculated exactly, e.g., by transfer matrix methods, or otherwise. Although factorization is not exact in 2D, typically it is a good approximation if performed properly and certainly for strong interactions. Rigorous results again follow.[26]

There are few experimental realisations of diffusion in 1D; quasi-one-dimensional properties occur for adsorption in carbon nanotubes, similarly for metals adsorbed on the $Si(111)5\times2$-Au structure.[27,28] In any case, our results also have implications for the validity of modeling of diffusion for 2D adsorbates. Even with the restriction to nearest neighbor interactions, there are many more choices for the kinetics in 2D. Thus the increased possibility of misinterpretation of features observed in the diffusivity—as due a larger set of interactions operating, as opposed to a particular kinetics. (The literature tends to emphasise the kinetics of initial-state interactions.) We also note that most analytical work[29] employing linear response theory disregards the dynamic correlations in Eq. (53). However, the net current is nonzero in 2D for any choice of kinetics and the use of the product form of D is a simplifying assumption that is factually incorrect so that the gradient expansion presented here is a viable alternative.[26]

As a final comment we note that the complete time evolution of an interacting adsorbate out of equilibrium of course demands a full diagonalization of the transition matrix, as done elsewhere.[15] Likewise, a full microscopic understanding of the hopping kinetics demands a quantum mechanical calculation of the transition probabilities coupled with the derivation of the master equation as done elsewhere for long jumps.[6,7]

ACKNOWLEDGMENTS

APPENDIX A

Here we present some details concerning the diffusion kinetics scenarios for interactions on the 1D lattice out to second neighbors. We write the generalization of Eq. (10) and a similar expression for $W_{i+1}^<(\mathbf{n})$ as

$$W_i^>(\mathbf{n}) = J_0 n_i(1-n_{i+1}) \sum_{n_k=0,1} D_{n_{i-2}n_{i-1}n_{i+2}n_{i+3}}\tilde{n}_{i-2}\tilde{n}_{i-1}\tilde{n}_{i+2}\tilde{n}_{i+3},$$

$$(A1)$$

$$W_{i+1}^<(\mathbf{n}) = J_0(1 - n_i)n_{i+1} \sum_{n_k=0,1} D_{n_{i+3}n_{i+3}n_{i-1}n_{i-2}}\tilde{n}_{i-2}\tilde{n}_{i-1}\tilde{n}_{i+2}\tilde{n}_{i+3},$$

$$(A2)$$

where $\tilde{n}_k = (1 - n_k)$ if $n_k = 0$ or $\tilde{n}_k = n_k$ if $n_k = 1$ and the subscripts of the D coefficients specify the occupation neighborhood of the hopping pair. Under a reflection of this neighborhood, 4 of the 16 coefficients have their subscript order unchanged and the other 12 are paired by detailed balance, giving 6 constraints. In terms of the interaction parameters $u_n = \exp(\beta V_n), (n = 1, 2), v = \exp(\beta V_t)$ the latter are

$$D_{0100} = u_1 u_2^{-1} D_{0010}, \quad (A3)$$

$$D_{1000} = u_2 D_{0001}, \quad (A4)$$

$$D_{1100} = u_1 v D_{0011}, \quad (A5)$$

$$D_{1010} = u_1^{-1} u_2^2 D_{0101}, \quad (A6)$$

$$D_{1110} = u_2 v D_{0111}, \quad (A7)$$

$$D_{1101} = u_1 u_2^{-1} v D_{1011}. \quad (A8)$$

The indexed coefficients introduced in Eq. (43) are then obtained by expansion of Eqs. (A1) and (A2). With $D_{0000} = 1$, we have, as examples, $A_1 = D_{0100} - 1, B_1 = D_{0010} - 1, A_{11} = D_{1100} - D_{0100}, C_{11} = D_{0110} - D_{0100} - D_{0010} + 1$, etc. Various interaction-based kinetics can be obtained by specifying the 6 coefficients appearing on the left hand side of Eqs. (A3)–(A8), as well as the three symmetric coefficients $D_{0110}, D_{1001}, D_{1111}$ which generate the free parameters $C_{11}, C_{1001}, C_{1111}$. The only constraint is that $\langle W \rangle \geq 0$. A necessary condition for particle-hole symmetry is that $D_{1111} = D_{0000} = 1$, which translates to

$$A_1 + B_1 + C_{11} + A_{11} + B_{11} + A_{111} + B_{111} + C_{1111} = 0$$

$$(A9)$$

the generalization of Eq. (12). Our three parent scenarios are:

(a) Initial state interactions. The D_{mnpq} are to reflect the effect of the neighbors on the hopping rate of the particle in its initial state only. The obvious choice is $D_{0100} = u_1$, $D_{1000} = u_2$, $D_{1100} = u_1 u_2 v$, $D_{1010} = u_2^2$, $D_{1110} = u_1 u_2^2 v$, $D_{1101} = u_1 u_2 v$, $D_{0110} = u_1 u_2$, $D_{1001} = u_2$, $D_{1111} = u_1 u_2^2 v$. The nonzero coefficients generated are $A_1 = u_1 - 1$, $B_1 = A_{10} = u_2 - 1$, $A_{11} = u_1(u_2 v - 1)$, $A_{101} = A_{10}^2$, $A_{111} = A_{11}A_{10}$, $C_{11} = A_1 B_1$.

(b) Final state interactions. The effect of neighbors on rate of the hopping particle jumping to its final state are the converse of those above. The corresponding choice is $D_{0100} = u_2^{-1}$, $D_{1000} = 1$, $D_{1100} = u_2^{-1}$, $D_{1010} = u_1^{-1}$, $D_{1110} = u_1^{-1} u_2^{-1}$, $D_{1101} = u_2^{-2}$, $D_{0110} = u_1^{-1} u_2^{-1}$, $D_{1001} = u_2^{-1}$, $D_{1111} = u_1^{-1} u_2^{-2} v^{-1}$. The standard coefficients mirror those for case (a) with the exchange of labels $A \leftrightarrow B$ and the inverse interaction parameters: $A_1 = B_{10} = u_2^{-1} - 1$, $B_1 = u_1^{-1} - 1$, $B_{11} = u_1^{-1}(u_2^{-1} v^{-1} - 1)$, $B_{101} = B_{10}^2$, $B_{111} = B_{11}B_{10}, C_{11} = A_1 B_1$.

(c) Initial and final state interactions. We choose to generalize the condition $A_1 = -B_1$, used for first neighbor interactions alone, to all of our standard coefficients, i.e. $A_{11} =$

$-B_{11}$, $A_{111} = -B_{111}$, etc. This gives the condition $D_{mnpq} + D_{pqmn} = 2$ for 5 of the 6 coefficients appearing in Eqs. (A3)–(A8); for the sixth we have $D_{1110} + D_{0111} = 2D_{0110}$. The three free coefficients then appear as

$$C_{11} = D_{0110} - 1, \quad (A10)$$

$$C_{1001} = D_{1001} - 1, \quad (A11)$$

$$C_{1111} = D_{1111} + D_{0110} - 2. \quad (A12)$$

If particle-hole symmetry is imposed then $C_{11} = C_{1111}$ and there are only two free parameters. The values set by our choice are

$$A_1 = (u_1 u_2^{-1} - 1)/(u_1 u_2^{-1} + 1), \quad (A13)$$

$$A_{10} = (u_2 - 1)/(u_2 + 1), \quad (A14)$$

$$A_{11} = (u_1 v - 1)/(u_1 v + 1) - A_1, \quad (A15)$$

$$A_{101} = (u_1^{-1} u_2^2 - 1)/(u_1^{-1} u_2^2 + 1) - A_{10} + A_1, \quad (A16)$$

$$A_{111} = (C_{11} + 1)(u_2 v - 1)/(u_2 v + 1) - A_{11}, \quad (A17)$$

$$A_{1101} = (u_1^{-1} u_2^2 - 1)/(u_1^{-1} u_2^2 + 1) + (u_1 u_2^{-1} v - 1)/(u_1 u_2^{-1} v + 1)$$
$$- A_{11}. \quad (A18)$$

APPENDIX B

Here we mention our method of calculating the equilibrium correlators on a 1D lattice and give the equations for the functions $H_\alpha = G_\alpha/F_\alpha$, which contribute in Eq. (50), in terms of them. The standard approach to obtain correlators is to maximize the system's (grand) canonical partition function, subject to the normalization constraints. The latter are just sums of correlators, here spanning three sites for interactions out to second neighbors; three of these are

$$\langle \bullet \bullet \rangle + \langle \bullet \circ \rangle = \langle \bullet \rangle = \theta, \quad (B1)$$

$$\langle \bullet \bullet \bullet \rangle + \langle \bullet \bullet \circ \rangle = \langle \bullet \bullet \rangle, \quad (B2)$$

$$\langle \circ \bullet \circ \rangle + \langle \bullet \bullet \circ \rangle = \langle \bullet \circ \rangle \quad (B3)$$

with three more obtained from these by exchange of particles and holes. Correlators spanning more than three sites must be factored in terms of these two- and three-site functions. Three additional relations are necessary to solve for the unknowns. As examples, we have

$$\frac{\langle \bullet \bullet \circ \rangle^2}{\langle \bullet \bullet \bullet \rangle \langle \circ \bullet \circ \rangle} = \exp(\beta V_2), \quad (B4)$$

$$\frac{\langle \bullet \bullet \bullet \rangle^3 \langle \bullet \circ \rangle^2}{\langle \bullet \bullet \circ \rangle^2 \langle \circ \bullet \circ \rangle \langle \bullet \bullet \rangle^2} = \exp[\beta\mu - \beta(2V_1 + 2V_2 + 3V_t)],$$

$$(B5)$$

$$\frac{\langle \bullet \circ \bullet \rangle^3 \langle \circ \bullet \circ \rangle \langle \circ \circ \rangle^2}{\langle \bullet \circ \circ \rangle^4 \langle \bullet \circ \rangle^2} = \exp[\beta\mu - 3\beta V_2]. \quad \text{(B6)}$$

The solution of these nonlinear equations is not always straightforward for large interaction strengths ($|\beta V| \gg 1$). For a numerically more robust and accurate method, especially for the coverage-derivatives of the correlators, we have employed the transfer matrix method to calculate the partition function.[17] Correlators spanning up to six sites are obtained with this method by using as a basis the states (occupancies) of a cell of three sites and constructing the matrix of Boltzmann weights for the particle interactions within and between two neighboring cells. The grand partition function is then obtained as the leading eigenvalue of this 8×8 matrix, with the coverage given as a derivative with respect to the chemical potential, μ. In practice $\theta(\mu, T)$, follows directly from the corresponding (left and right) eigenvector and the correlators by the contraction of derivatives of the transfer matrix with these eigenvectors.

Equations for the functions H_α, in terms of these correlators, are given below. The first of these is just a diagrammatic recasting of Eq. (48):

$$H_{4h} = \frac{d\langle \bullet \bullet \circ \rangle/d\theta}{\langle \bullet \bullet \circ \rangle} + \frac{d\langle \bullet \bullet \rangle/d\theta}{\langle \bullet \bullet \circ \rangle} + \frac{d\langle \circ \circ \rangle/d\theta}{\langle \bullet \circ \rangle}, \quad \text{(B7)}$$

$$H_{5h} = 2\frac{d}{d\theta}\ln\frac{\langle \bullet \bullet \bullet \rangle}{\langle \bullet \circ \bullet \rangle} + d\langle \bullet \bullet \rangle/d\theta\left[\frac{1}{\langle \bullet \bullet \circ \rangle} - \frac{1}{\langle \bullet \circ \rangle} - \frac{1}{\langle \bullet \bullet \rangle}\right], \quad \text{(B8)}$$

$$H_{52h} = H_{4h} - \frac{d}{d\theta}\ln\langle \bullet \circ \circ \bullet \rangle, \quad \text{(B9)}$$

$$H_{6h} = \frac{d}{d\theta}\ln\langle \bullet \bullet \bullet \bullet \bullet \bullet \rangle, \quad \text{(B10)}$$

$$H_{6h2} = H_{4h} + 2\frac{d}{d\theta}\ln\frac{\langle \bullet \circ \bullet \bullet \rangle}{\langle \bullet \circ \bullet \rangle}, \quad \text{(B11)}$$

$$H_{62h} = H_{52h} + H_{6h}, \quad \text{(B12)}$$

$$H_{63h} = \frac{d}{d\theta}\ln\frac{\langle \bullet \circ \bullet \circ \rangle^2}{\langle \bullet \circ \circ \bullet \rangle}. \quad \text{(B13)}$$

[1] W. Dieterich, P. Fulde, and I. Peschel, Adv. Phys. **29**, 527 (1980).

[2] A. R. Allnatt and A. Lidiard, Rep. Prog. Phys. **50**, 573 (1987).

[3] J. W. Haus and K. Kehr, Phys. Rep. **150**, 263 (1987).

[4] R. Gomer, Rep. Prog. Phys. **53**, 917 (1990).

[5] T. Ala-Nissila, R. Ferrando, and S. C. Ying, Adv. Phys. **51**, 949 (2002).

[6] M. Azzouz, H. J. Kreuzer, and M. R. A. Shegelski, Phys. Rev. Lett. **80**, 1477 (1998).

[7] M. Azzouz, H. J. Kreuzer, and M. R. A. Shegelski, Phys. Rev. B **66**, 125403 (2002).

[8] C. J. Chudley and R. J. Elliot, Proc. Phys. Soc. London **77**, 33 (1961).

[9] W. Zwerger, Z. Phys. B: Condens. Matter **42**, 333 (1981).

[10] L. Badowski, M. A. Zaluska-Kotur, and Z. W. Gortel, Phys. Rev. B **72**, 245413 (2005).

[11] K. Kawasaki, Phys. Rev. **145**, 224 (1966).

[12] R. Kikuchi, Suppl. Prog. Theor. Phys. **35**, 1 (1966).

[13] H. Sato and R. Kikuchi, Phys. Rev. B **28**, 648 (1983).

[14] Z. Chvoj, J. Phys.: Condens. Matter **12**, 2135 (2000).

[15] J.-S. McEwen, S. H. Payne, H. J. Kreuzer, and C. Bracher, Int. J. Quantum Chem. **106**, 2889 (2006).

[16] D. A. Reed and G. Ehrlich, Surf. Sci. **102**, 588 (1981).

[17] H. J. Kreuzer and S. H. Payne, in *Computational Methods in Colloid and Interface Science* (Dekker, New York, 1999).

[18] R. J. Glauber, J. Math. Phys. **4**, 294 (1963).

[19] H. J. Kreuzer, Langmuir **8**, 774 (1992).

[20] H. Singer and I. Peschel, Z. Phys. B: Condens. Matter **39**, 333 (1980).

[21] J.-S. McEwen, S. H. Payne, H. J. Kreuzer, M. Kinne, R. Deneke, and H.-P. Steinrück, Surf. Sci. **545**, 47 (2003).

[22] R. Kikuchi, in *Fast Ion Transport in Solids*, edited by E. van Gool (North Holland, Amsterdam, 1976), p. 555.

[23] S. Lapinskas, E. E. Tornau, V. E. Zubkus, and A. Rosengren, Surf. Sci. **414**, 44 (1998).

[24] M. A. Zaluska-Kotur and Z. W. Gortel, Phys. Rev. B **74**, 045405 (2006).

[25] S. H. Payne, H. J. Kreuzer, M. Kinne, R. Deneke, and H.-P. Steinrück, Surf. Sci. **513**, 174 (2002).

[26] S. H. Payne and H. J. Kreuzer (unpublished).

[27] T. Hasegawa and S. Hosoki, Phys. Rev. B **54**, 10300 (1996).

[28] A. Kirakosian, R. Bennewitz, F. J. Himpsel, and L. W. Bruch, Phys. Rev. B **67**, 205412 (2003).

[29] A. Danani, R. Ferrando, E. Scalas, and M. Torri, Int. J. Mod. Phys. B **11**, 2217 (1997).

[30] Here and elsewhere, some intermediate factorizations and manipulations of correlators are conveniently carried out in diagrammatic form.